



# Temporal-Spatial Profiling of Pedunculopontine Galanin-Cholinergic Neurons in the Lactacystin Rat Model of Parkinson's Disease

Joanna L. Elson<sup>1,2</sup> · Rafael Kochaj<sup>3</sup> · Richard Reynolds<sup>4</sup> · Ilse S. Pienaar<sup>4,5</sup>

Received: 15 May 2017 / Revised: 22 November 2017 / Accepted: 22 November 2017 / Published online: 7 December 2017  
© Springer Science+Business Media, LLC, part of Springer Nature 2017

## Abstract

Parkinson's disease (PD) is conventionally seen as resulting from single-system neurodegeneration affecting nigrostriatal dopaminergic neurons. However, accumulating evidence indicates multi-system degeneration and neurotransmitter deficiencies, including cholinergic neurons which degenerate in a brainstem nucleus, the pedunculopontine nucleus (PPN), resulting in motor and cognitive impairments. The neuropeptide galanin can inhibit cholinergic transmission, while being upregulated in degenerating brain regions associated with cognitive decline. Here we determined the temporal-spatial profile of progressive expression of endogenous galanin within degenerating cholinergic neurons, across the rostro-caudal axis of the PPN, by utilizing the lactacystin-induced rat model of PD. First, we show progressive neuronal death affecting nigral dopaminergic and PPN cholinergic neurons, reflecting that seen in PD patients, to facilitate use of this model for assessing the therapeutic potential of bioactive peptides. Next, stereological analyses of the lesioned brain hemisphere found that the number of PPN cholinergic neurons expressing galanin increased by 11%, compared to sham-lesioned controls, and increasing by a further 5% as the neurodegenerative process evolved. Galanin upregulation within cholinergic PPN neurons was most prevalent closest to the intra-nigral lesion site, suggesting that galanin upregulation in such neurons adapt intrinsically to neurodegeneration, to possibly neuroprotect. This is the first report on the extent and pattern of galanin expression in cholinergic neurons across distinct PPN subregions in both the intact rat CNS and lactacystin-lesioned rats. The findings pave the way for future work to target galanin signaling in the PPN, to determine the extent to which upregulated galanin expression could offer a viable treatment strategy for ameliorating PD symptoms associated with cholinergic degeneration.

**Keywords** Cholinergic co-expression · Galanin · Lactacystin · Parkinson's disease · Pedunculopontine nucleus

## Introduction

Galanin is a 29-amino acid (aa) long (30 aa long in humans) neuropeptide encoded for by the *GAL* gene (Tatemoto et al. 1983). It is widely distributed in the brains of rodents (Skofitsch and Jacobowitz 1985; Melander et al. 1986), non-human primates (Kordower et al. 1992), and humans (Le Maître et al. 2013; Gentleman et al. 1989), where it helps regulate several physiological processes, including aspects of cognition, food intake, nociception, and sexual behavior (Vrontakis 2002; Ogren et al. 2010). Expression levels of galanin and galanin receptors were shown to be altered in the brains of patients diagnosed with neurological disorders, including Alzheimer's disease (AD) (Beal et al. 1990) and multiple sclerosis (Wraith et al. 2009). In addition, a study by Chan-Palay (1988) showed that in AD post-mortem brains, severe hypertrophy affects a network of neuronal axons expressing galanin (especially those based within the anterior

✉ Ilse S. Pienaar  
I.S.Pienaar@sussex.ac.uk; i.pienaar@imperial.ac.uk

<sup>1</sup> Institute of Genetic Medicine, Newcastle University, Newcastle upon Tyne NE1 3BZ, UK

<sup>2</sup> Centre for Human Metabolomics, North-West University, Potchefstroom, South Africa

<sup>3</sup> Wolfson Centre for Age-Related Diseases, King's College London, Guys Campus, London SE1 1UL, UK

<sup>4</sup> Centre for Neuroinflammation and Neurodegeneration, Division of Brain Sciences, Faculty of Medicine, Imperial College London, W12 0NN, London, UK

<sup>5</sup> School of Life Sciences, University of Sussex, Sussex House, Falmer, Brighton BN1 9RH, UK

part of the nucleus basalis of Meynert (nbM)), which innervate the basal cholinergic neurons (termed hyperinnervation). Based on these findings, Alexandris et al. (2015) conducted post-mortem analyses of the nbM taken from patients who suffered from Lewy body disorders (LBD), but with no concurrent AD pathology, to calculate the innervation scores of fibers containing galanin. LBD is clinically separated into Parkinson's disease (PD), PD with dementia (PDD), and dementia with Lewy bodies (DLB), based on the severity of cognitive dysfunction a patient presents with, and on the temporal sequence by which cognitive- versus motor symptoms appear to manifest (Mrak and Griffin 2007). The study reported that in LBD patients, galanin innervation was increased, and that galanin expression occurred within the soma of neurons based in the nbM.

As indicated, studies suggest that an intricate functional relationship exists between galanin and the neurotransmitter acetylcholine (ACh) (Chan-Palay 1988; Crawley and Wenk 1989). However, conflicting findings have been reported as to whether galanin signaling benefits or acts deleteriously on the functioning and survival of cholinergic neurons in the brains of patients suffering from neurodegenerative disease. For instance, Counts et al. (2006) analyzed post-mortem anterior nucleus basalis samples taken from AD patients that had been categorized into three diagnostic groups, namely patients that had been diagnosed as having no cognitive impairment, those with mild cognitive impairment, and those with early-stage (mild/moderate) AD. Across the three subgroups of AD patients, the investigators detected no difference in the degree to which galanin-containing axons innervated remaining cholinergic basal forebrain neurons. In addition, the study reported that remaining cholinergic neurons within the nucleus basalis expressed mRNA for all three galanin receptor subtypes identified so far; however, similar levels were measured for all three diagnostic subgroups. Hence, this work showed that galanin-containing axons are not hypertrophied during the prodromal or early stages of AD, but that galanin fiber enlargement seems to rather manifest during late-stage AD, as reported previously (Chan-Palay 1988; Bowser et al. 1997). Hyperinnervation by such hypertrophied neurons may play a crucial role in regulating the cholinergic tone of the basocortical cholinergic system, the integrity which is structurally and functionally compromised in AD.

In other work, Steiner et al. (2001) reported that galanin overexpression impairs learning and memory in mice. The study's additional finding, that galanin overexpression associated with a significant reduction in the number of cholinergic neurons in these animals, suggests that galanin overexpression is harmful to the survival and function of cholinergic neurons. On the other hand, there is considerable support for the notion that galanin may counteract cholinergic degeneration, with Ding et al. (2006) who reported that galanin protects cholinergic basal forebrain neurons against AD-related amyloid- $\beta$

(A $\beta$ ) toxicity. The notion that galanin is neuroprotective was corroborated by Pironi et al. (2010), who demonstrated in cholinergic SN56 neuroblastoma cells that Gal2-11, a galanin receptor 2/3 subtype agonist, abolished A $\beta$ -induced apoptotic DNA fragmentation and that the neuroprotection was mediated through a reduction of caspase-3 mRNA expression. Similarly, in other work, Elliot-Hunt et al. (2011) showed that A $\beta_{1-42}$  peptide induced a significantly greater degree of cell death in mice harboring loss-of-function mutations in galanin or galanin receptor 2 (GAL2), and that this was reduced in galanin over-expressing transgenic mice, in each case compared to strain-matched wild-type control mice. In neonatal hippocampal neurons taken from these transgenic mice, exogenous galanin or Gal2-11 fully rescued deficits in galanin knock-out, but not in GAL2 cultures that lack a functional GAL2, confirming that galanin's protective effects are mediated by activation of GAL2. Taken together, several studies have demonstrated that both exogenous galanin and neuronal upregulation of galanin is neuroprotective against neurodegeneration, implying that development of galanin agonists might have a role as potential neuroprotective therapies against neurodegenerative disease.

Galanin is expressed within neurotransmitter inputs to the pedunculopontine nucleus (PPN), located in the caudal pontomesencephalic tegmentum of the rostral brainstem (Gai et al. 1993), where it regulates diverse functions, including locomotion (Moro et al. 2010; Pienaar et al. 2015a, b), cognitive functions such as attention, learning, and working memory (Taylor et al. 2004; Faure et al. 2014), as well as arousal and sleep-wake transitions (Datta and Siwek 2002; Hobson and Pace-Schott 2002). Although disruption of voluntary motor control, a prominent clinical feature of PD, is thought to be due to dopaminergic pathophysiology, evidence is growing that certain motor and non-motor comorbidities seen in PD patients are likely to arise from progressive degeneration of the cholinergic PPN (Hirsch et al. 1987; Rinne et al. 2008; Pienaar et al. 2013).

Considering the limited number of studies which have reported on galanin-cholinergic interactions in PD-affected brains, we made use of rats that had been intra-nigraly and unihemispherically lesioned with the irreversible ubiquitin proteasome system inhibitor, lactacystin. The lactacystin rat model recapitulates several neuropathological features of PD, including degeneration of the nigrostriatal system (Pienaar et al. 2015a, b) and PPN cholinergic neurons (McNaught et al. 2002; Pienaar et al. 2015a, b; Elson et al. 2016), intracytoplasmic accumulation of altered proteins within remaining neurons (McNaught et al. 2002; Pienaar et al. 2015a; Elson et al. 2016), PD-related motor abnormalities (Pienaar et al. 2015a, b; Elson et al. 2016), as well as an inflammatory reaction (Elson et al. 2016). The animals were grouped into those sacrificed at 8 days following surgery (acute stage) and those sacrificed at 35 days post-surgery (chronic stage), to

characterize the temporal- and spatial expression profile of intrinsic galanin, from the intra-nigral site of the toxin's injection, to then spread across the rostro-caudal axis of the PPN. We performed this extensive characterization in order to better understand whether an alteration of endogenous galanin expression could be regarded as a response to neurodegeneration of PPN cholinergic neurons, potentially aimed at preserving the remaining pool of such neurons.

## Materials and Methods

### Animals

Male, adult (250 g) Sprague-Dawley rats ( $n = 30$ ) were used for the current experiments and kept under controlled environmental conditions (24–25 °C; humidity 50–60%; 12 h dark/light cycle) with free access to tap-water and food. Imperial College London's ethics review panel accepted all experimental protocols, with all experiments that were performed in line with the Animals (Scientific Procedures) Act 1986 (UK).

### Surgeries and Pharmacological Validation of Nigral Lesion Size

Neurotoxic lactacystin lesions of the Substantia Nigra pars compacta (SNpc) were performed while the rats ( $n = 18$ ) were deeply anesthetized with Isoflurane (Isoflo Abbot Laboratories Ltd., UK), which was vaporized into O<sub>2</sub> and initiated at a delivery flow-rate of 2 L/min. Following the standard procedure for preparing the animal for surgery, the SNpc was stereotaxically injected as previously described (Pienaar et al. 2015a, b; Elson et al. 2016). In brief, a dental drill was used to drill a small burr hole through the cranium over the left SNpc, using the coordinates: 5.2 mm (anterior–posterior) and 2.4 mm (medio-lateral), relative to bregma (Paxinos and Watson 2009). Each rat in the lesioning group received 10 µg of lactacystin (Enzo Life Sciences, UK), dissolved in 2.5 µl isotonic sterile 0.9% saline (pH 7.4). A total of 4 µl of the lactacystin solution was infused into each rat. The solution was prepared immediately prior to delivery by diluting the stock solution, which was stored on ice to prevent degradation. The lactacystin dose given here is similar to that used in several other studies (e.g., Mackey et al. 2013; Vernon et al. 2010; Harrison et al. 2015; Pienaar et al. 2015a, b; Elson et al. 2016), and was well tolerated by the rats, resulting in no mortalities. Sham-lesioned rats ( $n = 12$ ) received an equal volume of sterile saline only.

The intra-nigral infusion was delivered via a blunt-tipped 10 µl (32-G) Hamilton glass syringe (700 series, VWR International, Denmark), at a rate of 1 µl/min, which was driven by a microinjector syringe pump (11 Plus Elite,

Harvard Apparatus, USA), at a depth of –7.6 mm (ventral-dural, relative to the dural surface of the brain). The needle was left in situ for an additional 5 min before slowly retracting from the brain. Aseptic conditions prevailed throughout all surgical procedures. Following surgery, the scalp was sutured and topical antibacterial ointment (Topazone, Austin Laboratories, Canada) was applied. The rats were left to fully recover in a heated recovery chamber, which included providing fluid replacement therapy, before being returned to their main cages. Analgesic (Meloxicam, 1 mg/kg intraperitoneally (i.p.), Boehringer Ingelheim, Germany) was administered daily until an animal had fully recovered, based on grooming and overall appearance, including having returned to their pre-surgery weight. Sutures were removed 7–10 days post-surgery.

In order to assess the efficacy of the lactacystin-induced SNpc lesion and to confirm the absence of SNpc damage in sham-lesioned animals, all rats were assessed for amphetamine-induced rotation bias at 7 days post-surgery. Testing was performed during the dark portion of the light cycle by an assessor blind to the treatment condition, so as not to introduce bias. In rats, systemic application of D-amphetamine enhances dopamine (DA) content at striatal dopaminergic nerve terminals (Robinson and Becker 1982). In turn, dose-dependent D-amphetamine-induces dose-dependent differences in DA content between the two cerebral hemispheres which in turn produces rotations away from the lesioned side, where the greatest level of DA signaling occurs (Glick et al. 1981). D-amphetamine (5 mg/kg, Sigma-Aldrich, UK) was administered i.p. to the rats at a dose of 1 ml/kg, dissolved in 0.9% sterile saline. At 30 min post-injection, an animal was placed in a Perspex circling bowl (height 360 mm, diameter 400 mm) and the net number of turns made in a contralateral and ipsilateral direction was counted over a 30-min period. Sham-lesioned control rats were similarly assessed to confirm the absence of a nigral lesion and sacrificed at similar time-points to that of the toxin-lesioned animals.

Rats were sacrificed either at 8 (Time (T)1) or 35 days (T2) following lesioning with the toxin (T1:  $n = 9$ , T2:  $n = 9$ ) or sham surgery (T1:  $n = 6$ , T2:  $n = 6$ ), via injection with a lethal dose of sodium pentobarbital (100 mg/kg, i.p.), before transcardial perfusion with 50 ml heparinized phosphate-buffered saline (PBS) at 37 °C, followed by 4% paraformaldehyde (PFA) in PBS (pH 7). Rats' brains were then removed, with each brain that was post-fixed in the same fixative solution for 48 h, followed by cryopreservation in 30% sucrose in PBS. The brains were then snap-frozen in isopentane that had been pre-chilled on dry ice and stored at –80 °C until serial cryostat sectioning at 30 µm thickness, in the coronal plane. The sections were thaw mounted onto Super Frost Plus histological slides (Fisher Scientific, USA) with slides stored at –80 °C until histological processing. Cresyl fast violet

(CFV) staining was used to confirm infusion needle placements, using staining procedures similar to those previously described (Elson et al. 2016; Pienaar et al. 2015a).

Lactacystin-lesioned rats were included in the study if D-amphetamine induced a minimum of 7 ipsilateral complete rotations/min. Out of 18 toxin-lesioned rats, 16 were selected for the present study, based on their ipsilateral D-amphetamine-induced rotation scores. Of these 16, a further 2 were excluded due to poor stereotaxic needle placement, according to the analysis of the CFV-stained brain sections. Therefore, the statistical analysis of the stereology data presented in the present study is based on a total of 14 lesioned rats (T1:  $n = 7$ , T2:  $n = 7$ ) and 12 sham-lesioned control ones (T1:  $n = 6$ , T2:  $n = 6$ ).

### Immunohistochemistry and Immunofluorescence

Dopaminergic neurons in the SNpc of both toxin- and sham-lesioned rats, sacrificed at both T1 and T2, were identified immunohistochemically by staining for the enzyme tyrosine hydroxylase (TH), the rate-limiting enzyme accountable for DA synthesis (reviewed by Daubner et al. 2011). The sections were dewaxed, hydrated, dehydrated, and mounted as previously described (Pienaar et al. 2015a, b). Similarly, the sections were incubated for 60 min at room temperature (RT) with a polyclonal primary antibody raised against TH (1:1000 anti-rabbit; Pel-Freez Biologicals, USA), diluted in 20% normal goat serum in PBS, followed by incubation with the secondary antibody (1:200, biotinylated goat anti-rabbit; Vector Laboratories, USA) for 2 h at RT. Antigen/primary-antibody complex binding was detected using a commercially available kit for detecting streptavidin–biotin–peroxidase substrate (Vectastain, Vector Laboratories, Burlingame, CA, USA) and visualized by applying 33'-diaminobenzidine (DAB, Vector Laboratories) for 8–10 min at RT.

Cholinergic neurons of the rat PPN were immunofluorescently double-stained for choline acetyltransferase (ChAT), the rate-limiting enzyme in the biosynthetic pathway for ACh (Lipton 1946) and for galanin. After drying out the sections overnight at RT, the sections were hydrated in a graded ethanol (EtOH) series and then washed in distilled water. Endogenous peroxidase was quenched for 20 min by exposing the sections to 0.3%  $H_2O_2$  in 0.1 M tris-buffered saline (TBS). Antigen retrieval was performed by heating the sections for 5 min in boiled citric acid buffer solution (2 mM/L citric acid, 9 mM/L trisodium citrate dehydrate, pH 6.0), followed by applying 10% normal donkey serum to the sections for 60 min at RT, to block non-specific binding. The blocking solution was discarded before the primary antibodies were simultaneously applied for detecting ChAT- (1:150 polyclonal goat, AB144P; Invitrogen, USA) and galanin-immunoreactive (ir) neurons (1:2000 polyclonal rabbit, AB2233; Merck Millipore, USA). The sections were left to

incubate overnight in the antibody solution at 4 °C. The following day, the sections were washed in PBS ( $3 \times 5$  min) before incubating for 2 h at RT in a solution containing the secondary antibodies. These were Alexa Fluor 568-conjugated donkey anti-goat (1:200, Vector Laboratories) for identifying ChAT-ir neurons and Alexa Fluor 488-conjugated donkey anti-rabbit (1:200, Vector Laboratories) for revealing galanin-ir ones. The sections were then immersed for 5 min in a freshly filtered solution of 0.5% Sudan Black B (Sigma-Aldrich, UK), prepared as a saturated solution in 70% EtOH (Pienaar et al. 2015c). Sudan Black B treatment is a widely used method by which to reduce autofluorescence (Oliveira et al. 2010). Sections were then rinsed under running tap water, followed by a final rinse in PBS ( $3 \times 5$  min), before mounting under a coverslip using an aqueous mounting medium containing the nuclear dye 4',6-diamidino-2-phenylindole (DAPI) (DAKO, Germany). For all stains, negative control sections from each animal underwent identical staining preparation, except that the primary or secondary antibodies were omitted. All antibody and serum dilutions were made in TBS.

To evaluate the quality of the immune reactions and allow for consistency between batches of stained brain tissue sections, at least two stained slides per reaction (TH and ChAT-galanin-DAPI) per animal were visually inspected with the aid of either an optical microscope (for viewing TH-stained sections) or confocal imaging (for viewing ChAT-galanin-DAPI-stained sections). To further ensure that the antibody binding was specific, microscope-aided visual inspection was carried out for each animal on two negative control slides, one where the primary antibody had been omitted, while the secondary antibody had been omitted in the other.

High-magnification ( $\times 20$  air-immersion objective lens) photomicrographs was captured with a digital camera (Optronics,  $1200 \times 1660$  pixels) coupled to an AxioImager M2 microscope (Carl Zeiss Ltd., Heidelberg, Germany) of the TH-stained sections. The images were recorded using a charge-coupled device (CCD) color video camera ( $1200 \times 1660$  pixels, Optronics, Goleta, CA, USA), fitted with a zoom lens and linked to a desktop computer. The captured images were saved with Northern Eclipse image software (v8.0, Empix Imaging Inc., Mississauga, Canada). Analysis at high magnification (Fig. 1a) revealed that in the SNpc of control rats, TH-ir neurons that had been immunolabeled using the DAB-peroxidase system presented with a brown immunopositive soma as well as axonal and dendritic processes, similar to previous reports (Nair-Roberts et al. 2008). Figure 1a is a representative image of a DAB-stained brain section showing the SNpc of a sham-lesioned control rat.

PPN rat brain sections where cholinergic neurons have been co-stained for galanin and counterstained with DAPI were viewed with a TCS SP5 II confocal laser scanning microscope (Leica Microsystems, Wetzlar, Germany) under  $\times 20$  magnification. The images were digitally viewed with LAS

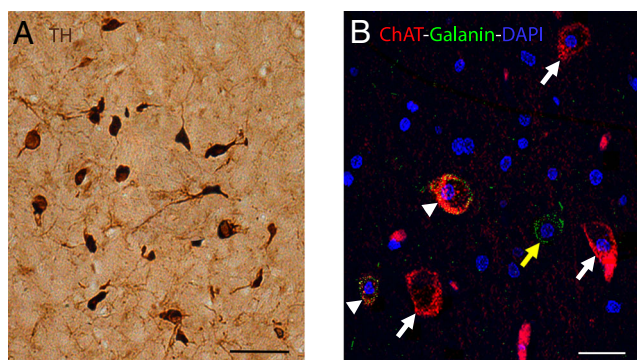


**Fig. 1** **a** Representative high-power-magnified microscopic images taken with a  $\times 20$  air-immersion objective lens of TH-ir neurons within the SNpc of a sham-lesioned control rat. DAB served as the chromogen, which is seen here as brown cytoplasmic staining. Scale bar: 50  $\mu\text{m}$ . **b** An overlay image consisting of a composite average of z-series stacks, collected using confocal microscopy equipped with a  $\times 20$  objective lens, showing the PPN of a representative lactacystin-lesioned rat. The image reveals ChAT- (red) and galanin-ir (green) neurons, with co-labeled neurons appearing as yellow/orange. Sections were counterstained with DAPI (blue) to visualize nuclei within PPN neurons. White arrow heads represent individual neurons immunoreactive for both ChAT and galanin, with galanin immunoreactivity that surrounds the nucleus, corresponding to the perikaryal cytoplasm. White arrows indicate PPN cholinergic neurons containing no galanin, while the yellow arrow shows a galanin-ir neuron within the PPN, which was immunonegative for ChAT, and hence a PPN non-cholinergic neuron. Scale bar: 20  $\mu\text{m}$

EZ image analysis software (Leica Microsystems) and merged automatically using built-in functions in Adobe Photoshop (version 7.0). Figure 1b shows a representative digital image of a fluorescently stained ChAT-galanin-DAPI PPN brain section, derived from a lactacystin-lesioned rat. The reaction for the ChAT-galanin neurons overlapped completely (an unquantified observation). Clear galanin-immunoreactivity was only observed in lactacystin-lesioned animals, with very low levels of galanin-immunoreactivity that was seen in the PPN of rats that had not been lesioned with the neurotoxin; these observations are reflected in the stereology results presented below. Interestingly, a subpopulation of neuronal cells expressing galanin did not co-express ChAT (Fig. 1b), indicating galanin localization within non-cholinergic neurons of the PPN to further contribute to the notion of the PPN as a highly heterogeneous structure. This aspect will be discussed further below.

### Stereological Neuronal Counts

To quantify ChAT-ir neurons that co-localized with galanin-ir ones in the rat PPN and also to determine the number of TH-ir neurons in the SNpc of the rat brains, the unbiased optical fractionator method for stereological cell quantification was used (West et al. 1991). Stereological estimates were made in the lesioned and non-lesioned brain hemispheres within the structures of interest (SNpc and PPN) of lactacystin-

lesioned rats compared to sham-lesioned control rats, using a computer-based stereology software system (Image-Pro® Plus, Media Cybernetics, Rockville, USA) attached to a Nikon Eclipse E800 motorized microscope and a live video camera (JVC 3CCD KY-F55B; JVC Ltd., Yokohama, Japan). The SNpc was distinguished from the substantia nigra pars reticulata (SNr), the ventral tegmental area (VTA), and the retrorubral area by consulting published guidelines on anatomical landmarks and regional differences in cell density orientation (Baquet et al. 2009; Oorschot 1998; Paxinos and Watson 2009). In the sham-lesioned rats, the PPN was identified on the ChAT-stained sections by the PPN's characteristic wedge-like shape, formed by the Ch5 cholinergic neuronal population (Mesulam et al. 1983, 1989). Due to neuronal loss, this shape was disrupted in toxin-lesioned rats; however, sufficient numbers of cholinergic neurons remained to form a recognizable cholinergic neuronal nucleus. Anatomical landmarks that provided additional guidance to identify the PPN (Paxinos and Watson 2009). In this regard, the PPN's rostral boundary consists of the SNr, with the PPN that extends dorso-caudally toward the lateral tip of the superior cerebellar peduncle, at  $60^\circ$  from a vertical line (Pienaar and Van de Berg 2013; Mena-Segovia et al. 2009). The PPN-Ch5 cell group was distinguished from a neighboring cholinergic cell group (Ch6), which defines the laterodorsal tegmental nucleus (LDTg), by referring to a rat brain atlas (Paxinos and Watson 2009).

Of every 6th section, a tiled image was taken at  $\times 4$  magnification. In this image, the ipsilateral and contralateral SNpc and PPN were delineated manually. The total area of the counting frames, relative to the area of the respective area of interest (AOI), provides the area sampling fraction (asf). Using the uniform systematic random sampling method with a sampling fraction of 2, the computer system placed counting frames ( $140 \times 160 \mu\text{m}$ ) across the whole of the AOI. The number of TH-ir neurons in each of the counting frames was then counted at  $\times 10$  magnification, whereas the ChAT-galanin-ir neurons were counted at  $\times 20$  magnification. To eliminate edge effects, “acceptance” and “forbidden” lines were used: Cells crossing either the east or north borders were included in the count, whereas cells crossing either the south or west borders were ignored. The height of the sampling fraction (hsf) was calculated for each section by using a microcator (MT-12, Heidenhain, Germany), which measures the average height of the counted optical plane relative to the section thickness. For each section, the number of TH-ir and ChAT-ir neurons was then calculated using the equation  $N = n(1/ssf)(1/asf)(1/hsf)$ , where  $n$  equals the number of positive cells counted and  $ssf$  refers to the section sampling fraction. In our case, the  $ssf$  was  $1/6$ , as we analyzed every 6th section throughout the AOI.

## Statistical Analyses

Statistical analyses were performed by using the Statistical Package for Social Sciences (SPSS) software programme (Version 20, IBM Corp., Chicago, USA) with the limit for statistical significance set at 0.05. The following *P* value designations were applied: \*\*\**P* < 0.001, extremely significant; \*\**P* ≤ 0.01, highly significant; \**P* ≤ 0.05, significant; and *P* > 0.05, non-significant (n/s). For analyzing the SNpc TH-ir neuronal stereology data, a one-way ANOVA was applied to compare the neuronal densities counted within the PPNs of the two brain hemispheres in the different treatment groups, representing both assessment time-points, followed by a Tukey post-hoc comparison. A two-way ANOVA followed by a Tukey post-hoc comparison test was used for analyzing the PPN ChAT-ir neuronal stereology data to consider for the effects of time and distance away from the SNpc on the sham- and toxin-lesioned rats. The results are expressed as the mean value ± the standard error of the mean (SEM).

## Results

### Validation of the Dopaminergic Nigrostriatal Lesion

At 30 min following D-amphetamine administration, 16 out of 18 lactacystin-lesioned animals rotated exclusively in an ipsiversive direction. These 16 rats were then randomly divided into 2 groups, those representing an acute stage (*n* = 7 (121 ± 23 complete turns)), and those representing a chronic stage (*n* = 7 (114 ± 15 complete turns)) of experimental parkinsonism, at which respective time-point the brains were collected for stereological evaluation.

None of the sham-lesioned rats (*n* = 12) revealed biased D-amphetamine-induced rotational behavior post-surgery. Stereological neuronal counts of TH-ir SNpc for sham-lesioned control rats sacrificed at the first time-point (*n* = 6) revealed similar SNpc dopaminergic neuronal counts between the two hemispheres (ipsilateral side: 11,742 ± 378; contralateral side: 11,976 ± 296; Fig. 2 (Ai, B)), translating to a very small overall inter-hemispheric difference of 1.95% (*P* = 0.83, n/s; Fig. 2(B)). Similarly, at the chronic assessment time-point (*n* = 6), difference between the control rats' stereological TH-ir neuronal counts in the ipsilateral (13,151 ± 239) and contralateral SNpc (13,241 ± 239) accounted for only a 0.68% difference (n/s, *P* = 0.99; Fig. 2 (Aii, B)).

In lactacystin-lesioned rats sacrificed at the acute time-point (*n* = 7), the non-injected hemisphere's SNpc contained 11,704 ± 164 TH-ir neurons, while the toxin-injected SNpc contained only 7276 ± 227 TH-ir neurons, the inter-hemispheric difference of 37.98%, which represented a statistically significant neuronal loss (\*\*\**P* < 0.0001; Fig. 2 (Ai, B)). At the chronic time-point (*n* = 7), a highly significant

TH-ir neuronal loss was again detected between the two hemispheres (\*\*\**P* < 0.0001; Fig. 2 (Aii, B)), with a density count of 11,568 ± 229 for the SNpc on the non-injected hemispheric side compared to 6467 ± 390 on the toxin-injected hemispheric side, representing a difference of 44.1%. A comparison between the TH-ir neuronal densities of the injected hemispheric side of toxin-lesioned rats, culled at 8 and 35 days post-surgery, did not reveal a statistically significant difference (*P* = 0.149, n/s).

Taken together, the data suggests that in this in vivo rat model of PD, a rapid loss of SNpc TH-ir neurons occurs within a short time-period following the intra-nigral infusion of lacytacystin, with a relatively stable population of resistant neurons that remained, subsequent to the initial insult and up to 35 days following the intra-nigral toxin infusion.

### Stereological Cell Counts and Topological Distribution Profile of PPN ChAT-ir Neurons

The panel of images shown in Fig. 3 of ChAT-ir neurons in the PPN under both toxin and sham-control conditions represent progressively posterior anatomical levels along the rostro-caudal axis of the PPN. The images illustrate the significantly greater overall loss of such neurons at the later stage of the lesion, compared to the acute stage. The images also show that this greater loss of ChAT-ir PPN neurons which were noted to have occurred at the later time following the lesion is largely due to time-dependent spreading of the lactacystin-induced damage and destruction of neurons. Thus, lactacystin decreases the number of PPN ChAT-ir neurons located in the most rostral (nearest to the intra-nigral injection site) PPN region, to then gradually also impact upon the cholinergic neurons of the medial and (even later) the caudal PPN sections.

Stereological cell counts were made of the ChAT-ir PPN neurons on the ipsilateral and contralateral hemispheric sides in the lactacystin- and sham-lesioned rat brains at both time-points. On the ipsilateral hemispheric side of control rats culled at the "acute" assessment stage (*n* = 6), 3130 ± 43 neurons were recorded, with 3154 ± 44 on the contralateral hemispheric side. As to the rats where the sham lesion was allowed to progress up to 35 days post-surgery (*n* = 6), the density values of cholinergic neurons were ipsilateral hemisphere, 3029 ± 51 and contralateral hemisphere, 3062 ± 53. In contrast, the following ChAT-ir neuronal densities were recorded in toxin-lesioned rats' PPN: ipsilateral hemisphere: 2475 ± 38; contralateral hemisphere: 3005 ± 80 (acute stage, *n* = 7); ipsilateral hemisphere: 2017 ± 70; contralateral hemisphere: 3050 ± 50 (chronic stage, *n* = 7).

In sham-lesioned rats, a two-way ANOVA detected no statistically significant difference between ipsilateral and contralateral PPN ChAT-ir neuronal counts when the data sets that represent either the first (*n* = 6) or the second post-surgical

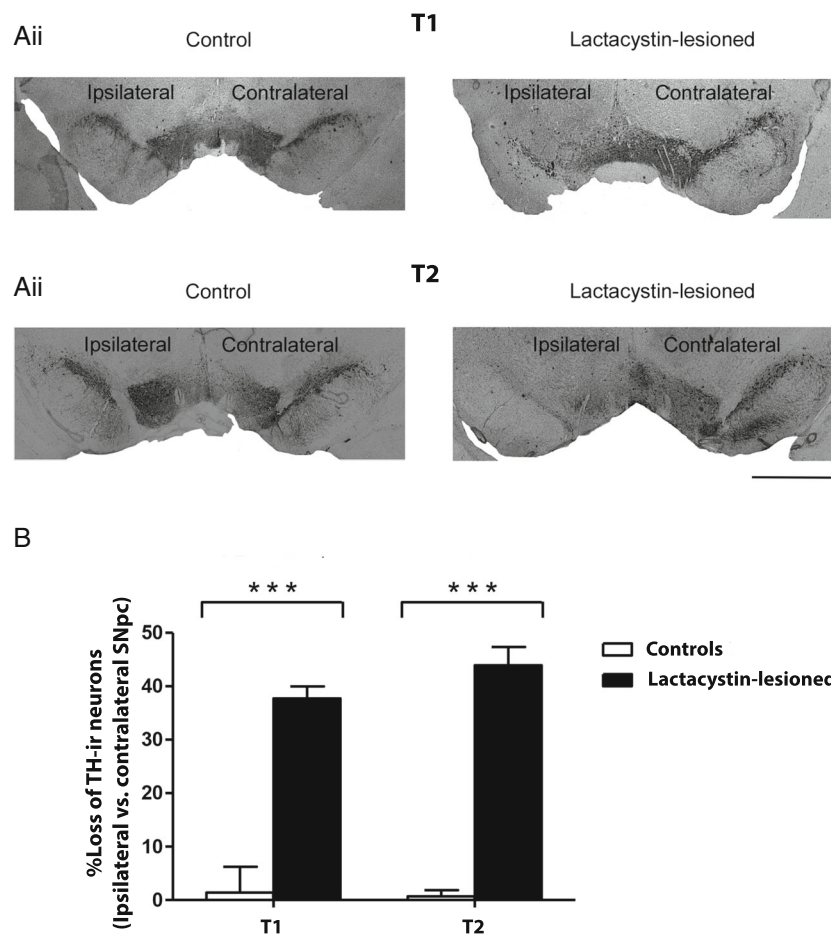


**Fig. 2** (Ai) A representative photomicrograph of a midbrain coronal section showing lactacystin-induced partial (38%) inter-hemispheric loss of SNpc TH-ir neurons at 8 (Aii) and 35 days post-surgery (44% neuronal loss) with the SNr and VTA that also showed some toxin-induced neuronal damage. The loss of TH-ir neurons occurs on the side ipsilateral (left) to the stereotaxic needle infusion of lactacystin, with no cell loss observed in the contralateral (right) SNpc. Typically, most damage occurred in closest proximity to the location of the needle tip. The degree of TH-ir neuronal loss was less but non-uniform further away from the needle tract. The representative image taken of the sham-lesioned control

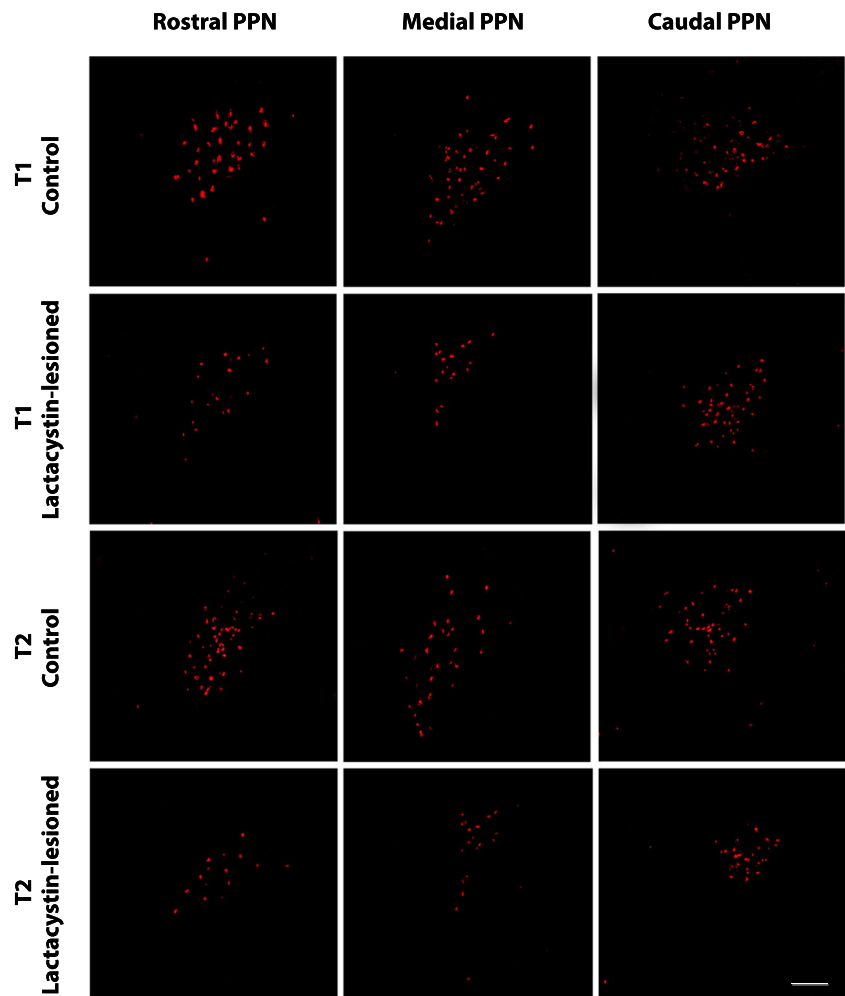
animal reveals a negligible inter-hemispheric loss of TH-ir neurons at either (Ai) 8 or (Aii) 35 days post-surgery. Images were captured with a  $\times 4$  028 NA air objective lens. Scale bar: 20  $\mu$ m. (B) Stereological quantification of TH-ir SNpc neurons reveal neuronal loss unihemispheric to the intra-nigral injection site in all toxin-lesioned rats that was statistically extremely significant at both the first ( $***P = 0.89$ ) and second time-point ( $***P = 0.99$ ) compared to SNpcs of control rats. Greater TH-ir neuronal loss was seen in lactacystin-lesioned rats at the latter time-point, suggesting a time-dependent progression of the lesion

evaluation time-point ( $n = 6$ ) were considered (Fig. 4a). On the other hand, for the lactacystin-lesioned rats, a highly significant difference ( $***P < 0.0001$ ) was seen in terms of cholinergic neuronal loss when the ipsilateral and contralateral hemispheres were compared at the earlier ( $n = 7$ ) and also the later time-point ( $n = 7$ ) (Fig. 4a).

Previous work that analyzed the topological distribution profile of ChAT-ir neurons in the non-lesioned (intact) PPN of rats revealed a characteristic rostro-caudal density gradient, with a higher density of such neurons seen in the caudal segments of the nucleus compared to the rostral ones (Mena-Segovia et al. 2009; Pienaar et al. 2015a, b; Elson et al. 2016). Similar to these reports, the current study revealed an overall significant effect when a comparison was drawn between the cholinergic neuronal density values of the PPN from

the most rostral sections, transitioning to the caudal end of the nucleus ( $***P < 0.0001$ ). Time (in days) since surgery produced no significant effect on the regular ChAT-ir neuronal density pattern in the sham-lesioned rats ( $P = 0.97$ , n/s). To investigate the effect of the toxin, the ipsilateral (injected) hemisphere of the lactacystin-lesioned rats was compared to the sham-lesioned ones by applying a section-by-section analysis, i.e., for the acute lesion cohort: section (S)1 of lactacystin-lesioned rats compared to S1 of sham-lesioned ones; for the chronic lesion cohort: S1 of lactacystin-lesioned rats compared to S1 of sham-lesioned rats, etc. (Fig. 4b, see insert). Analysis done on the ipsilateral PPN ChAT-ir neuronal densities of rats sacrificed at the first assessment time-point revealed that S1 and S2 ( $***P < 0.0001$ ), S3 ( $*P = 0.039$ ), and S4 ( $***P < 0.0001$ ) differed significantly

**Fig. 3** Low-magnification photomicrographs ( $\times 10$  magnification) of fluorescently-tagged ChAT-ir PPN neurons of rats lesioned with either lactacystin vehicle or the toxin and then sacrificed at 8 or 35 days post-surgery. The images were obtained from a single optical section. Scale bar: 300  $\mu\text{m}$ . These representative images of control and lesioned rats illustrate that the lesion mainly affected the most rostral segments of the PPN at 8 days post-lesion, while at 35 days post-lesion, lactacystin impacted upon ChAT-ir neuronal viability across the rostro-caudal extent of the PPN



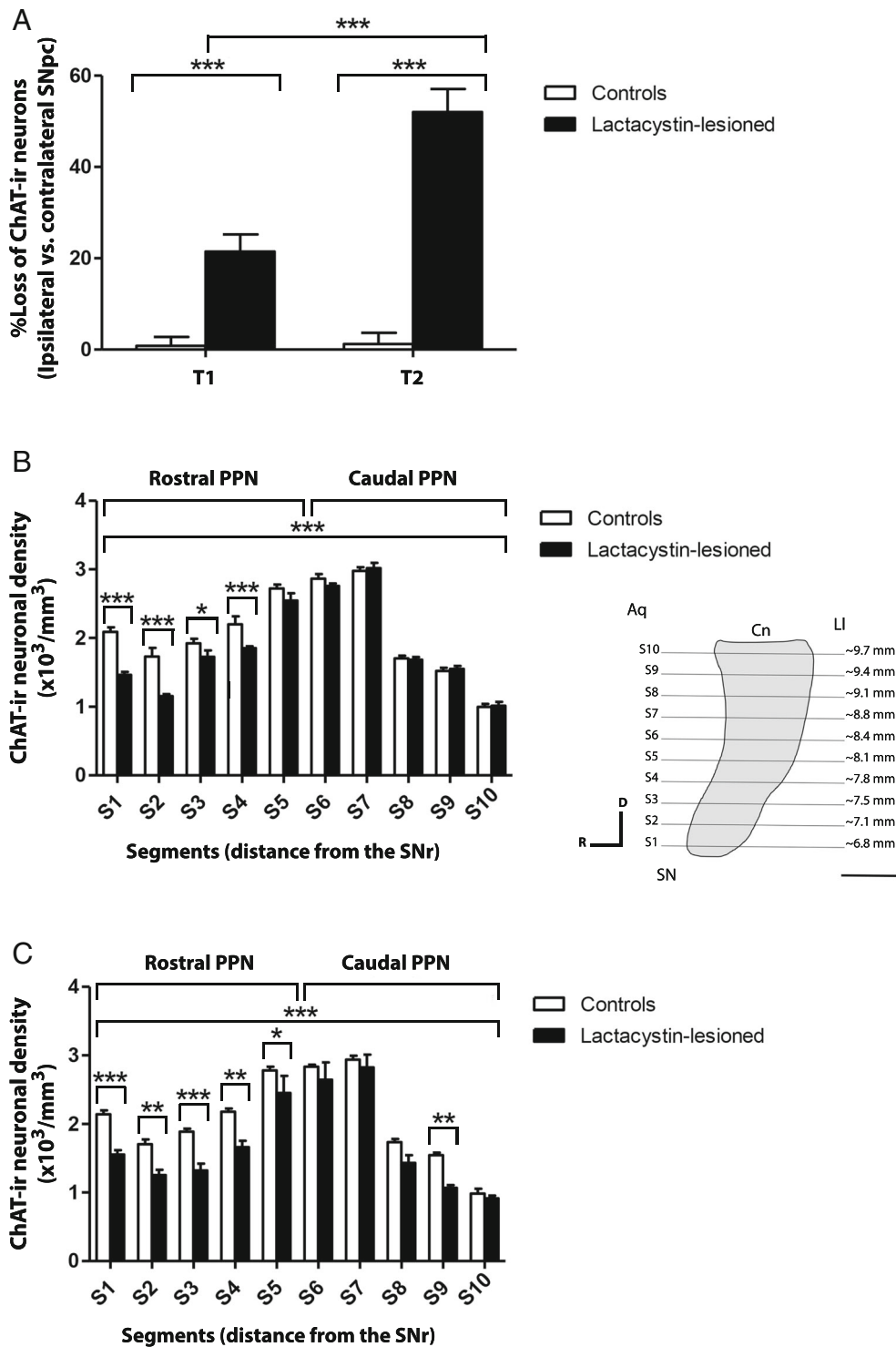
between sham control and toxin-lesioned rats with S5 ( $P = 0.068$ , n/s) showing a value of borderline significance. None of the more caudal sections ( $> S5$ ) showed a notable difference in neuronal density between the two rat groups (Fig. 4b). However, in rats that had been sacrificed 35 days following toxin injection, the following differences were recorded: S1 ( $***P = 0.0001$ ), S2 ( $**P = 0.007$ ), S3 ( $***P = 0.0001$ ), S4 ( $**P = 0.002$ ), S5 ( $*P = 0.046$ ), S6 ( $P = 0.066$ , n/s), and S9 ( $**P = 0.004$ ) (Fig. 4c), indicating that, as time since lesioning progresses, the toxin impacts upon the more caudal PPN segments in rats.

### Stereological Cell Counts and Topological Distribution Profile of PPN ChAT-Galanin-ir Neurons

The representative low-magnification microscopic image shown in Fig. 5, taken of neurons that had been dual immunofluorescently stained for ChAT and galanin, revealed the relatively sparse ChAT-galanin co-expressing neurons in the rat PPN, under non-toxic conditions. However, the images reveal the dramatic upregulation of the number of PPN

cholinergic neurons co-expressing galanin in the lactacystin rat model of PD, compared to sham-lesioned controls. The densities of ChAT- and galanin-ir co-expressing neurons were examined in both the non-lesioned contralateral and lesioned ipsilateral hemispheres of the lactacystin- and control rats for both assessment time-points. As expected, similar neuronal densities were seen on the non-injected/contralateral hemispheric sides of sham- (acute stage ( $n = 6$ ):  $314 \pm 7$ ; chronic stage ( $n = 6$ ):  $272 \pm 10$ ) compared to lactacystin-lesioned rats (acute stage ( $n = 7$ ):  $283 \pm 7$ ; chronic stage ( $n = 7$ ):  $299 \pm 12$ ) for both assessment time-points, the difference in each case being statistically n/s (acute stage:  $P = 0.14$ , n/s; chronic stage:  $P = 0.72$ , n/s) (Fig. 6a). In contrast, analysis of ChAT-galanin-ir neuronal densities of the PPN on the sham/lactacystin injected hemispheric side revealed significant differences when comparing sham- (acute stage ( $n = 6$ ):  $325 \pm 6$ ; chronic stage ( $n = 6$ ):  $301 \pm 11$ ) to toxin-lesioned rats (acute stage ( $n = 7$ ):  $532 \pm 15$ ; chronic stage ( $n = 7$ ):  $534 \pm 30$ ), revealing extremely statistically significant differences for both assessment time-points ( $***P < 0.0001$ ; Fig. 6a). However, from the first to the second lesion development time-point, a





slightly lower, but not notable, overall decrease of PPN ChAT-galanin-ir neuronal densities was measured on the lesioned hemispheric sides of toxin-lesioned rats ( $P = 0.42$ , n/s; Fig. 6a).

A section-by-section pair-wise comparison was conducted between the lactacystin- and sham-lesioned rats, i.e., S1 of sham controls sacrificed 8 days post-surgery versus S1 of

toxin-lesioned rats sacrificed at the same time-point, etc. For rats culled at the first time-point, analysis between the two groups revealed an extremely significant difference (S1–6) ( $***P < 0.0001$ ) that was especially prominent between the most rostral PPN sections, while a significant difference was also seen between the two groups for a more caudal section, namely S7 ( $*P = 0.025$ ; Fig. 6b). No significant differences

**Fig. 4 a** In serial sections taken from the brains of lactacystin intranigally injected rats or sham-lesioned controls, unbiased stereological cell counts revealed a significant inter-hemispheric loss of ChAT-ir PPN neurons at both 8 ( $***P < 0.0001$ ) and 35 days ( $***P < 0.0001$ ) post lactacystin-lesion. Neuronal counts are expressed as percentage cell loss on the injected hemispheric side relative to the non-injected hemispheric side, in the same treatment group. **b** The typical topographical distribution pattern of ChAT-ir neurons in the non-lesioned rat PPN at 8 days post-surgery, with the toxin that had the greatest effect on ChAT-ir neuronal counts in more rostral PPN segments. A segment-by-segment analysis, comparing sham- to lactacystin-lesioned rats, revealed the following comparisons to be statistically significant: S1 and S2 ( $***P < 0.0001$ ), S3 ( $*P = 0.039$ ), and S4 ( $***P < 0.0001$ ). The insert is a schematic of the rostro-caudal segmentation of the PPN (S1–S10) in the coronal plane which allowed for segment-by-segment comparisons of galaninergic- and cholinergic neurons to be made between the rats (sham- versus lactacystin-lesioned and rats sacrificed at T1 versus those at T2). This method is similar to that utilized in our previous work (Pienaar et al. 2015a, b; Elson et al. 2016) to assess the expression abundance of histological markers within PPN neurons across the rostro-caudal axis of the PPN. A view is shown of the PPN at  $-7.92$  mm from Bregma, according to a commonly used stereotaxic atlas (Paxinos and Watson 2009), with the approximate positions of major anatomical landmarks which provided guidance during sectioning of the PPN. *Aq* aqueduct, *Cn* cuneiform nucleus, *Ll* lateral lemniscus, *SN* substantia nigra. Scale bar: 300  $\mu$ m. **c** A comparison of the rat groups at 35 days post-surgery revealed that the lesion affected the entire extent of the PPN, although the effects were most prominent in rostral segments nearest to the intra-nigral injection site. A segment-by-segment analysis, comparing sham- to lactacystin-lesioned rats, revealed the following comparisons to be statistically significant: S1 ( $***P = 0.0001$ ), S2 ( $**P = 0.007$ ), S3 ( $***P = 0.0001$ ), S4 ( $**P = 0.002$ ), S5 ( $*P = 0.046$ ), and S9 ( $**P = 0.004$ )

were recorded for any of the most caudal sections (S8–10), suggesting that PPN regions that lie furthest away from the intra-nigral lesion site had not been stimulated to produce the neuropeptide galanin.

The stereology data of lactacystin-lesioned rats that had been sacrificed at the later time-point of 35 days post-surgery also showed highly significant differences when comparing sham- to toxin-lesioned rats. These differences were particularly prominent for the most rostral sections, with the values representing S1 and S2 which were significantly up-regulated in the lesioned rats compared to corresponding segments of sham-lesioned rats ( $***P < 0.0001$ ; Fig. 6c). None of the other sections further along the rostro-caudal length of the PPN showed any striking differences in terms of number of co-expressing neurons between lesioned and non-lesioned rats. However, galanin upregulation persisted within the most rostral segments, although less so compared to that seen at 8 days post-lesion. In contrast, a similar analysis was conducted to examine the level of co-expression within the ipsilateral hemispheres of the lactacystin-lesioned rats at both time-points (Figs. 6b, c). This revealed statistically significant differences between S1–6 ( $***P < 0.0001$ ) as well as S7 ( $**P = 0.007$ ). As was expected, no significant differences were detected between any of the segments in the sham-lesioned rats.

This reveals that the intra-nigally administered lactacystin injection that adversely affected cholinergic neurons, resulting in cholinergic cell death (Fig. 4a), induces transient upregulation of galanin within PPN cholinergic neurons soon after sustaining the lesion, with this effect diminishing substantially at 5 weeks following the surgery.

## Discussion

An animal model where rats are intracerebrally injected with lactacystin, a microbial metabolite isolated from *Streptomyces lactacystinaeu*, has shown promise for being instrumental in unraveling the molecular basis of PD, for testing novel therapeutics and for improving existing anti-PD ones (reviewed by Bentea et al. 2017). By binding to and inhibiting specific catalytic subunits of the proteasome, lactacystin could determine cell fate and cellular morphology (Orlowski 1999). Here we used two separate time-points for characterizing the progression of lactacystin-induced neuronal changes within the rat SNpc and PPN. The first time-point (T1) was at a relatively short period of time following the intra-nigral lesion, to represent an acute phase of lesion development, upon which the rats were sacrificed and the brains collected for histological evaluation at 8 days post-surgery. T2 represented the second time-point at which a separate set of rats were sacrificed at 35 days (5 weeks) post-surgery, thereby representing the chronic effects of exposure to the toxin. On the ipsilateral cerebral hemispheres of toxin-lesioned animals, at 8 days post-surgery, the toxin had induced a dramatic loss of TH-ir SNpc neurons. From this point onwards, the nigral lesion progressed relatively slowly for the next 4 weeks. The greatest PPN cholinergic neuronal loss occurred between the acute and chronic stage, with these results that may suggest that SNpc dopaminergic and PPN cholinergic neurons inherently have differential sensitivities to lactacystin. Differential cytotoxic responses were shown in our earlier work, with an intranigral infusion of lactacystin that induced cell death of both cholinergic and non-cholinergic neurons within the PPN; however, the non-cholinergic neurons showed increased resistance to the toxic insult (Elson et al. 2016). Hence, although this data confirms that the toxin is non-specific with regards to neuronal type, it suggests strongly that its impact to induce dopaminergic and cholinergic neuronal death follows a different time course, possibly due to the activation of different molecular signaling pathways. It therefore remains to be discovered how and which specific signal transduction pathways are preserved to a greater or lesser extent when exposed to the toxin in different neuronal populations.

As signaling molecules, neuropeptides participate in modulating synaptic neurotransmission, with galanin signaling occurring through transmembrane G-protein coupled receptors (GPCRs) (Branchek et al. 2000). Studies remain sparse on

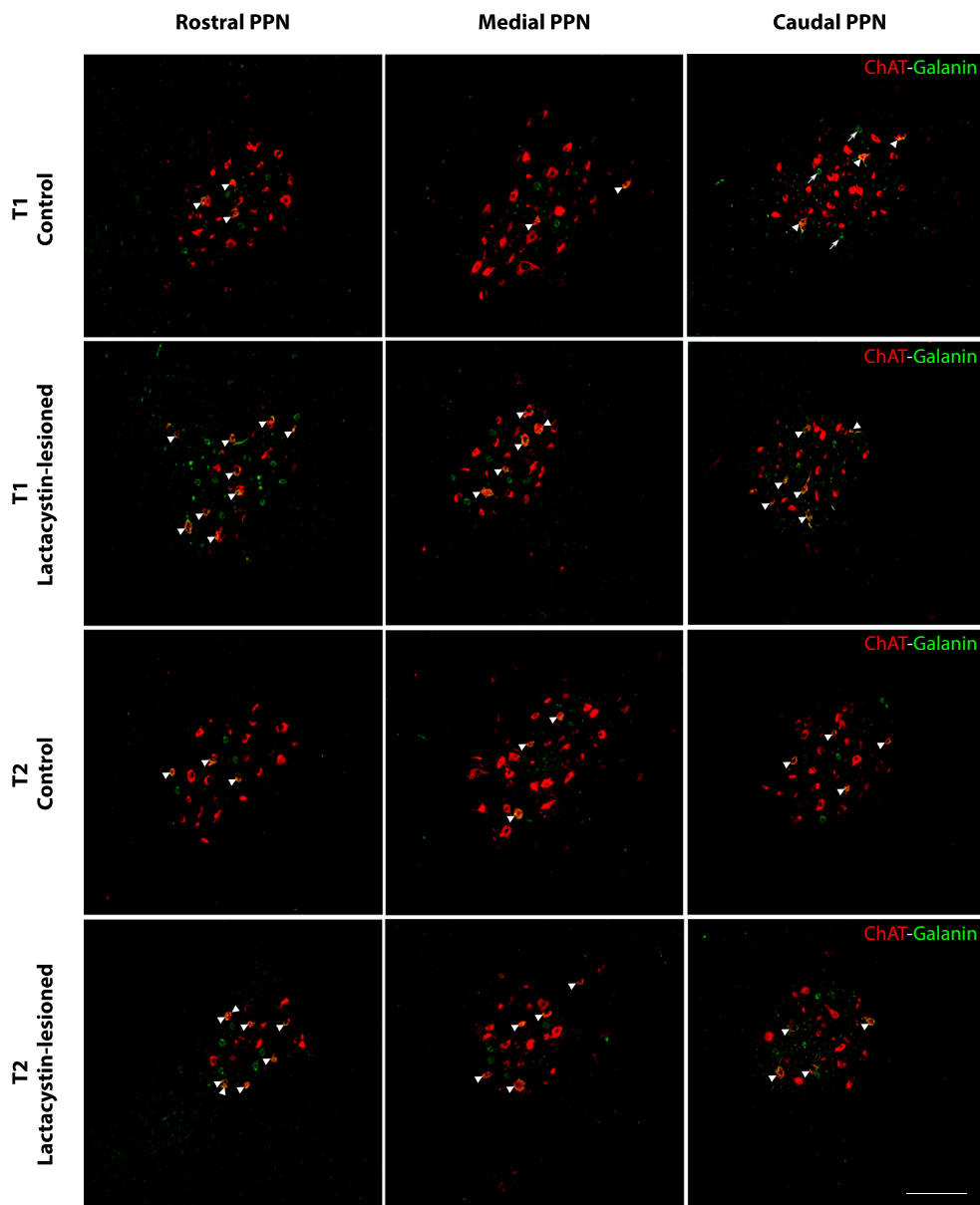


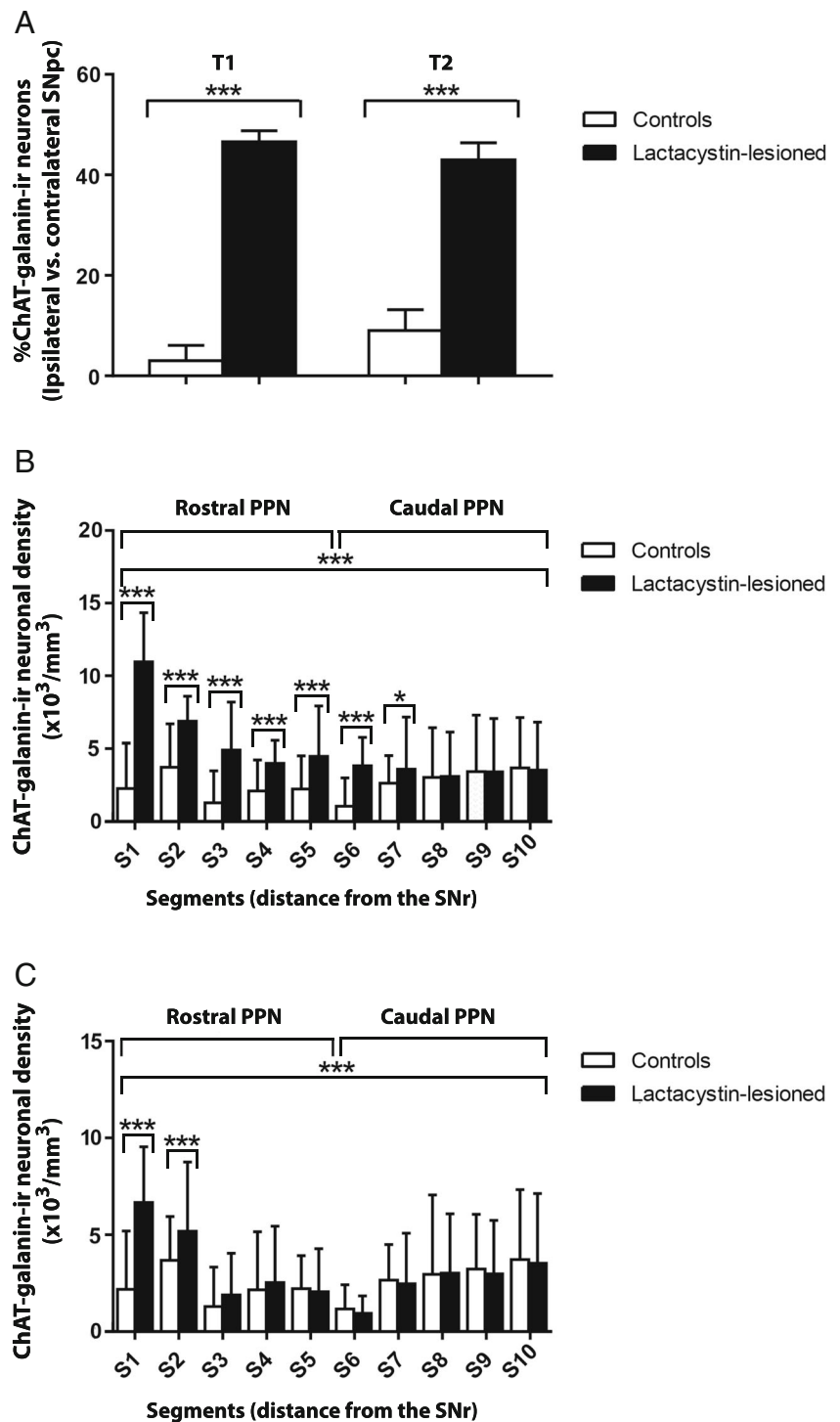
**Fig. 5** Low-magnification photomicrographs ( $\times 10$  magnification) taken of brain sections containing the PPN, showing the hemispheric side ipsilateral to the intra-nigral infusion. Sections were immunofluorescently double-stained for ChAT (red) and galanin (green), with representative example images (obtained from a single optical section) shown of the rostral, medial, and caudal levels of the PPN. Digital superimposition of the two color channels shows the colocalized areas (orange to yellow). Arrow heads indicate ChAT-ir galanin-ir neurons. Although the vast majority of ChAT-ir neurons were galanin-immunonegative under both toxic and control conditions, increased numbers of ChAT-

galanin-ir neurons were seen in the PPN of rats lesioned with lactacystin compared to sham controls, reflected in the stereological counts. Some galanin-ir neurons did not co-localize with ChAT-ir PPN ones (arrows). This was observed under both lactacystin and sham conditions but more so in the lactacystin-lesioned rats. In the PPN region on the lesioned side of toxin-treated rats, densely arranged galanin-ir fibers in close proximity to galanin-ir cell bodies was observed during both the acute and chronic assessment time-points. Galanin-ir nerve fiber formations were observed far less frequently than in lesioned rats. Scale bar: 500  $\mu\text{m}$

whether galanin expressing neurons are affected during progressive PD. Here we reveal, for the first time, that galanin upregulation occurs within cholinergic neurons in which cell death pathways have been activated due to the stereotaxic intra-nigral infusion of lactacystin. Specifically, examination of the stereological distribution data for rats representing T1

revealed that the toxin-induced lesion adversely affected survival of the PPN cholinergic neurons, but that only such neurons locating to the rostral segments of the nucleus, closest to the lesion site, underwent cell death. In sham-lesioned rats, galanin expression within this cholinergic neuronal population was unaffected by exposure to the toxin at either time-point

**Fig. 6 a** An extremely significant upregulation in the number of PPN cholinergic neurons co-expressing galanin was seen in lactacystin-lesioned rats at both time-points, with no data to suggest that such galanin upregulation was maintained from T1 to T2. Very low levels of such double-stained neurons were seen in the PPN of sham-lesioned rats. **b** ChAT-galanin-ir neuronal numbers within the ipsilateral PPN were upregulated in lactacystin-lesioned rats, this effect being most prevalent within the most rostral sections of the PPN. A segment-by-segment analysis, comparing sham- to lactacystin-lesioned rats, revealed the following comparisons to be statistically significant: S1–6 ( $***P < 0.0001$ ) and S7 ( $*P = 0.025$ ). **c** Topographical distribution of ChAT-galanin-ir PPN neurons for the later assessment time revealed only mild galanin upregulation in toxin-lesioned rats, which restricted to the most rostral PPN, closest to the SNpc injection site. Galanin levels within cholinergic neurons normalized, similar to sham-lesioned rats' levels, in the medial to most caudal PPN segments. Segmental analysis, comparing sham- to lactacystin-lesioned rats, revealed that both S1 and S2 were statistically different ( $***P < 0.0001$ )



and remained low, in line with previous studies reporting on immunohistological mapping of this peptide in non-toxic states (Skofitsch and Jacobowitz 1985; Melander et al. 1986).

When the stereology data on the PPN was arranged topographically, from nearest to furthest away from the intra-nigral lesion site, this section-by-section comparison showed that galanin is upregulated within PPN cholinergic neurons in response to the toxin. In particular, acute toxicity (T1) induced

over expression of galanin in the PPN cholinergic neurons with this upregulation that proceeded as far as S7, compared to sham-lesioned rats. At the more caudal ends of the nucleus (furthest away from the intra-nigral lesion site), similar numbers of cholinergic neurons expressed galanin than control rats, to further imply that acute toxin exposure exerted minimal lethal effects on ChAT-galanin co-expressing neurons. In contrast, at the more advanced stage of lesion development

(T2), as evidence by a greater overall loss of TH- (Fig. 2(B)) and ChAT-ir neurons (Fig. 4a), galanin retained upregulation within PPN cholinergic neurons, but at significantly lower levels than was seen at the acute time-point. The finding of this transient upregulation of galanin within toxin-challenged PPN cholinergic neurons, with this change in expression levels being restricted to segments nearest to the direct insult, indicates that galanin fulfills a neuroregulatory role in PPN cholinergic neurons' response to an irreversible ubiquitin proteasome system inhibitor, with a disturbance to the mitochondrial membrane potential and excessive oxidative stress that eventuates to apoptotic cell death (Zhou et al. 2010). In this regard, Cordero-Llana et al. (2014) revealed the importance of galanin for brain plasticity and repair with exogenous galanin resulting in upregulation of several pro-survival/pro-neuronal signaling pathways.

For ongoing characterization of the promising lactacystin rat model of PD, as was used in the current study, for mimicking the neuropathology impacting on the PPN during progressive PD, future work should continue to develop and validate behavioral test batteries for assessing both motor and non-motor aspects relating to the neurodegeneration of the different groups of neurons in the PPN. Particular emphasis should be placed on developing readout tools to functionally record from the PPN cholinergic neurons, with these neurons being especially vulnerable during progressive PD (Hirsch et al. 1987; Rinne et al. 2008; Pienaar et al. 2013), which the lactacystin rat model replicates (Pienaar et al. 2015a, b; Elson et al. 2016).

Measures such as reference- and working memory tasks for assessing the intactness of recognition memory (Okada et al. 2015), and also spatial memory, as is assessed in the Morris water maze (Baxter et al. 2013), have been validated for interrogating the basal forebrain cholinergic neurons. Similar strides are required for developing rodent behavioral measures that show a clear correlation between the PPN's cholinergic neurons, and a rodent's performance in this task. Subjection of lactacystin-lesioned rodents in which galanin has genetically been manipulated to be overexpressed, through the creation of transgenic rodent lines (for examples, see Pope et al. 2010; Zhang et al. 2012), to such optimized behavioral paradigms, will allow for rescue experiments to determine the capacity of galanin to restore PPN cholinergic functions which are severely disrupted in PD patients (reviewed by Müller and Bohnen 2013).

The current study also reports on the interesting observation that a distinct galaninergic population of neurons that do not express ChAT, an immunohistochemical marker of cholinergic neurons in the CNS, thus rendering them non-cholinergic, appears to increase in number within the PPN in this particular neurotoxin model of PD. Although this phenomenon was not quantified in the present study, the observation highlights interesting speculation and scope for future studies

to conduct an in-depth investigation as to the neurochemical identity of the neurons in which galanin displays upregulated expression following lactacystin lesioning, and how the spatial and temporal profiles alter as a result of such neurotoxicity.

The PPN is composed of a rich diversity of neuronal cell-types, with three major neurochemically distinct neuronal groups that have been identified in the PPN, namely cholinergic, GABA (gamma-aminobutyric acid)-ergic, and glutamatergic neurons, which are heterogeneously distributed along its rostro-caudal axis (reviewed by Pienaar et al. 2016). Glycine immunoreactivity was also reported to be present in the human PPN (Pienaar et al. 2013), as well as in various other vertebrate species (Fort et al. 1993; Mineff et al. 1998). To further characterize the functional properties of the identified non-cholinergic galaninergic population of PPN neurons, future studies should characterize their neurochemical phenotypes in full, as the nature of this interaction between neuropeptides and neurotransmitters in a brain system can modulate synaptic neurotransmission by influencing presynaptic neurotransmitter release, receptor trafficking and recycling, as well as post-synaptic signal coupling (Salio et al. 2006). Related to this, although the axons of non-cholinergic neurons are more restricted in terms of length and number of collaterals, future work should also determine how they connect with other brain regions, such as the basal ganglia, thalamus, cortex, and spinal cord, in normal and pathological conditions. It is possible that such identified non-cholinergic galaninergic PPN neurons could also co-express other neuropeptides. An example of this is somatostatin, to form part of somatostatinergic brainstem neurons, which were shown to form afferent projections to the medial pre-optic nucleus, involved in regulating a variety of neuroendocrine processes, vegetative functions, sexual behavior, and for modulating the somato-motor system (Giehl and Mestres 1995). In this regard, future studies to explore the relative co-expression levels of galanin with other neuropeptides within non-cholinergic PPN neurons, and to characterize the temporal-spatial profile of such co-expression during progressive neurodegeneration, as seen in the lactacystin rat model of PD, are warranted.

The lactacystin rat model used here is an established rat model of PD that reflects clinical PPN neuronal damage to a remarkably accurate extent (Pienaar et al. 2015a). Using this rat model of PD, our current findings indicate that galanin expression levels could play a potentially important role in determining clinical manifestations of PD that associate with PPN cholinergic neuronal death, which include motor dysfunctions (e.g., gait dysfunction) as well as neuropsychiatric disturbances, such as those affecting cognition (reviewed by Pienaar et al. 2016). Thus far, studies focusing on galanin-ACh interactions have primarily done so within the context of AD. Considering that the PPN is a major source of cholinergic afferents, and that the nucleus is becoming a prominent target site for deep brain stimulation (DBS) as a means for

controlling PD-associated gait difficulties and postural disturbances (Plaha and Gill 2005; Mazzpone et al. 2005; Ferraye et al. 2010), it is surprising that only a limited number of studies thus far have explored whether galanin upregulation differs in PPN cholinergic neurons, as a result of PD. Our results suggest that galanin receptors could be considered potential targets for the development of novel anti-parkinsonian therapies. With rodent models being critical tools for furthering understanding as to the causes of PD, as well as for identifying novel therapeutics for treating the disease, characterizing galanin-cholinergic interactions in response to neurotoxins associated with PD, remains critical.

The current work highlights the need for further investigations aimed at better understanding the role of galanin in neuroprotecting PPN cholinergic neurons against PD-related toxin-mediated cell death and identify the mechanisms by which this may be achieved. Lactacystin binds and inhibits specific catalytic subunits of the proteasome to induce apoptosis (Orlowski 1999). However, the mechanism by which it induces such a cell fate remains a topic of considerable investigation. Some studies suggest that this occurs by way of stimulating the expression of the death protease, caspase-3 (Li et al. 2015), while others revealed that lactacystin triggers a conformational change of B cell lymphoma 2 (Bcl-2)-associated X (Bax) protein and that the anti-apoptotic counterpart to Bax (members of the Bcl-2 family) can prevent apoptosis by inhibiting the conformational change affecting Bax (Lang-Rollin et al. 2005).

The current study and our previous work (Pienaar et al. 2015a, b) demonstrated that lactacystin offers a suitable model for mimicking the neuropathology affecting the PPN in PD. For investigating the consequences of increased expression of galanin, and in order to determine if such protein upregulation could be deemed neuroprotective against PD-relevant PPN cholinergic neuronal death, future experiments should explore for differential expression and changes in the activity of apoptosis regulatory markers such as caspase-3, Bax, and Bcl-2. Future work should also consider the interacting pathways between galanin receptor signaling's downstream effects and lactacystin-induced impaired regulation of protein turnover, oxidative stress, mitochondrial dysfunction, and the central role that  $\alpha$ -synuclein is deemed to play in these processes, which converge to cause neuronal dysfunction and ultimately cell death in PD-affected brains and in animal model of the disease. In this regard, studies to determine for changes in the expression of the galanin receptors GalR1, GalR2, and GalR3 within cholinergic neurons of the PPN during the lactacystin-induced lesion's progression could reveal if galanin receptor signaling represent next-generation therapeutic targets for the treatment of PD.

**Acknowledgements** This study received grant support from the British Pharmacological Society and the Rosetrees Trust, awarded to ISP.

#### Compliance with ethical standards

**Conflict of Interest** The authors declare that they have no conflict of interest.

**Abbreviations** ACh, acetylcholine; AD, Alzheimer's disease; Aa, amino acid; A $\beta$ , amyloid- $\beta$ ; AOI, area of interest; Bcl-2, B-cell lymphoma 2; Bax, Bcl-2-associated X; ChAT, choline acetyltransferase; CFV, Cresyl fast violet; DAB, 3,3'-diaminobenzidine; DAPI, 4',6-diamidino-2-phenylindole; DBS, deep brain stimulation; DLB, dementia with Lewy bodies; DA, dopamine; EtOH, ethanol; GAL, galanin [gene]; GAL2, galanin receptor 2; GABA, gamma-aminobutyric acid; GPCRs, G-protein coupled receptors; Ir, immunoreactive; i.p., intraperitoneal; LDTg, laterodorsal tegmental nucleus; LBD, Lewy body disorders; NbM, nucleus basalis of Meynert; PFA, paraformaldehyde; PD, Parkinson's disease; PDD, PD with dementia; PPN, pedunculopontine nucleus; PBS, phosphate-buffered saline; RT, room temperature; SNpc, substantia nigra pars compacta; SNr, substantia nigra pars reticulata; T, time; TBS, tris-buffered saline; TH, tyrosine hydroxylase; VTA, ventral tegmental area

#### References

- Alexandris A, Liu AK, Chang RC, Pearce RK, Gentleman SM (2015) Differential expression of galanin in the cholinergic basal forebrain of patients with Lewy body disorders. *Acta Neuropathol Commun* 3(1):77. <https://doi.org/10.1186/s40478-015-0249-4>
- Baquet ZC, Williams D, Brody J, Smeyne RJ (2009) A comparison of model-based (2D) and design-based (3D) stereological methods for estimating cell number in the substantia nigra pars compacta (SNpc) of the C57BL/6J mouse. *Neuroscience* 161(4):1082–1090. <https://doi.org/10.1016/j.neuroscience.2009.04.031>
- Baxter MG, Bucci DJ, Gorman LK, Wiley RG, Gallagher M (2013) Selective immunotoxic lesions of basal forebrain cholinergic cells: effects on learning and memory in rats. *Behav Neurosci* 127(5):619–627. <https://doi.org/10.1037/a0033939>
- Beal MF, MacGarvey U, Swartz KJ (1990) Galanin immunoreactivity is increased in the nucleus basalis of Meynert in Alzheimer's disease. *Ann Neurol* 28(2):157–161. <https://doi.org/10.1002/ana.410280207>
- Bentea E, Verbruggen L, Massie A (2017) The proteasome inhibition model of Parkinson's disease. *J Parkinsons Dis* 7(1):31–63. <https://doi.org/10.3233/JPD-160921>
- Bowser R, Kordower JH, Mufson EJ (1997) A confocal microscopic analysis of galaninergic hyper-innervation of cholinergic basal forebrain neurons in Alzheimer's disease. *Brain Pathol* 7(2):723–730. <https://doi.org/10.1111/j.1750-3639.1997.tb01058.x>
- Brancheck TA, Smith KE, Gerald C, Walker MW (2000) Galanin receptor subtypes. *Trends Pharmacol Sci* 21(3):109–117. [https://doi.org/10.1016/S0165-6147\(00\)01446-2](https://doi.org/10.1016/S0165-6147(00)01446-2)
- Chan-Palay V (1988) Galanin hyperinnervates surviving neurons of the human basal nucleus of Meynert in dementias of Alzheimer's and Parkinson's disease: a hypothesis for the role of galanin in accentuating cholinergic dysfunction in dementia. *J Comp Neurol* 273(4):543–557. <https://doi.org/10.1002/cne.902730409>
- Cordero-Llana O, Rinaldi F, Brennan PA, Wynick D, Caldwell MA (2014) Galanin promotes neuronal differentiation from neural progenitor cells in vitro and contributes to the generation of new olfactory neurons in the adult mouse brain. *Exp Neurol* 256:93–104. <https://doi.org/10.1016/j.expneurol.2014.04.001>
- Counts SE, Chen EY, Che S, Ikonovic MD, Wu J, Ginsberg SD, Dekosky ST, Mufson EJ (2006) Galanin fiber hypertrophy within

- the cholinergic nucleus basalis during the progression of Alzheimer's disease. *Dement Geriatr Cogn Disord* 21(4):205–214. <https://doi.org/10.1159/000090906>
- Crawley JN, Wenk GL (1989) Co-existence of galanin and acetylcholine: is galanin involved in memory processes and dementia? *Trends Neurosci* 12(8):278–282. [https://doi.org/10.1016/0166-2236\(89\)90003-9](https://doi.org/10.1016/0166-2236(89)90003-9)
- Datta S, Siwek DF (2002) Single cell activity patterns of pedunculopontine tegmentum neurons across the sleep-wake cycle in the freely moving rats. *J Neurosci Res* 70(4):611–621. <https://doi.org/10.1002/jnr.10405>
- Daubner SC, Le T, Wang S (2011) Tyrosine hydroxylase and regulation of dopamine synthesis. *Arch Biochem Biophys* 508(1):1–12. <https://doi.org/10.1016/j.abb.2010.12.017>
- Ding X, MacTavish D, Kar S, Jhamandas JH (2006) Galanin attenuates beta-amyloid (Abeta) toxicity in rat cholinergic basal forebrain neurons. *Neurobiol Dis* 21(2):413–420. <https://doi.org/10.1016/j.nbd.2005.08.016>
- Elliot-Hunt CR, Holmes FE, Hartley DM, Perez S, Mufson EJ, Wynick D (2011) Endogenous galanin protects mouse hippocampal neurons against amyloid toxicity in vitro via activation of galanin receptor-2. *J Alzheimers Dis* 25:455–462
- Elson JL, Yates A, Pienaar IS (2016) Pedunculopontine cell loss and protein aggregation direct microglia activation in parkinsonian rats. *Brain Struct Funct* 221(4):2319–2341. <https://doi.org/10.1007/s00429-015-1045-4>
- Faure JB, Maques-Carneiro JE, Akimana G, Cosquer B, Ferrandon A, Herbeaux K, Koning E, Barbelivien A, Nehlig A, Cassel JC (2014) Attention and executive functions in a rat model of chronic epilepsy. *Epilepsia* 55(5):644–653. <https://doi.org/10.1111/epi.12549>
- Ferraye MU, Debu B, Fraix V, Goetz L, Ardouin C, Yelnik J, Henry-Lagrange C, Seigneuret E, Piallat B, Krack P, le Bas JF, Benabid AL, Chabardes S, Pollak P (2010) Effects of pedunculopontine nucleus area stimulation on gait disorders in Parkinson's disease. *Brain* 133(1):205–214. <https://doi.org/10.1093/brain/awp229>
- Fort P, Luppi PH, Jouver M (1993) Glycine immunoreactive neurons in the cat brain stem reticular formation. *Neuroreport* 4(9):1123–1126
- Gai WP, Blumbergs PC, Geffen LB, Blessing WW (1993) Galanin-containing fibers innervate substance P-containing neurons in the pedunculopontine tegmental nucleus in humans. *Brain Res* 618(1):135–141. [https://doi.org/10.1016/0006-8993\(93\)90436-Q](https://doi.org/10.1016/0006-8993(93)90436-Q)
- Gentleman SM, Falkai P, Bogerts B, Herrero MT, Polak JM, Roberts GW (1989) Distribution of galanin-like immunoreactivity in the human brain. *Brain Res* 505(2):311–315. [https://doi.org/10.1016/0006-8993\(89\)91458-3](https://doi.org/10.1016/0006-8993(89)91458-3)
- Giehl K, Mestres P (1995) Somatostatin-mRNA expression in brainstem projections into the medial preoptic nucleus. *Exp Brain Res* 103(3):344–354
- Glick SD, Weaver LM, Meibach RC (1981) Amphetamine enhancement of reward asymmetry. *Psychopharmacology* 73(4):323–327. <https://doi.org/10.1007/BF00426459>
- Harrison IF, Crum WR, Vernon AC, Dexter DT (2015) Neurorestoration induced by the HDAC inhibitor sodium valproate in the lactacystin model of Parkinson's is associated with histone acetylation and up-regulation of neurotrophic factors. *Br J Pharmacol* 172(16):4200–4215. <https://doi.org/10.1111/bph.13208>
- Hirsch EC, Graybiel AM, Duyckaerts C, Javoy-Agid F (1987) Tegmental loss in the pedunculopontine tegmental in Parkinson disease and in progressive supranuclear palsy. *Proc Natl Acad Sci U S A* 84(16):5976–5980. <https://doi.org/10.1073/pnas.84.16.5976>
- Hobson JA, Pace-Schott EF (2002) The cognitive neuroscience of sleep: neuronal systems consciousness and learning. *Nat Rev Neurosci* 3(9):679–693. <https://doi.org/10.1038/nrn915>
- Kordower JH, Le HK, Mufson EJ (1992) Galanin immunoreactivity in the primate central nervous system. *J Comp Neurol* 319(4):479–500. <https://doi.org/10.1002/cne.903190403>
- Lang-Rollin I, Maniati M, Jabado O, Vekrellis K, Papantonis S, Rideout HJ, Stefanis L (2005) Apoptosis and the conformational change of Bax induced by proteasomal inhibition of PC12 cells are inhibited by bcl-xL and bcl-2. *Apoptosis* 10(4):809–820. <https://doi.org/10.1007/s10495-005-0378-5>
- Le Maître E, Barde SS, Palkovits M, Diaz-Heijtz R, Hökfelt TG (2013) Distinct features of neurotransmitter systems in the human brain with focus on the galanin system in locus coeruleus and dorsal raphe. *Proc Natl Acad Sci U S A* 110(6):E536–E545. <https://doi.org/10.1073/pnas.1221378110>
- Li Y, Gao H, Wang Y, Dai C (2015) Investigation the mechanism of the apoptosis induced by lactacystin in gastric cancer cells. *Tumour Biol* 36(5):3465–3470. <https://doi.org/10.1007/s13277-014-2982-x>
- Lipton MA (1946) Mechanism of the enzymatic synthesis of acetylcholine. *Fed Proc* 5(1 Pt 2):145
- Mackey S, Jing Y, Flores J, Dinelle K, Doudet J (2013) Direct intranigral administration of an ubiquitin proteasome system inhibitor in rat: behavior, positron emission tomography, immunohistochemistry. *Exp Neurol* 247:19–24. <https://doi.org/10.1016/j.expneurol.2013.03.021>
- Mazzone P, Lozano A, Stanzione P, Galati S, Scarnati E, Peppe A, Stefani A (2005) Implantation of human pedunculopontine nucleus: a safe and clinically relevant target in Parkinson's disease. *Neuroreport* 16(17):1877–1881. <https://doi.org/10.1097/01.wnr.0000187629.38010.12>
- McNaught KSP, Bjorklund LM, Belizaire R, Isacson O, Jenner P, Olanow CW (2002) Proteasome inhibition causes nigral degeneration with inclusion bodies in rats. *Neuroreport* 13(11):1437–1441. <https://doi.org/10.1097/00001756-200208070-00018>
- Melander T, Hökfelt T, Rökaeus A (1986) Distribution of galanin-like immunoreactivity in the rat central nervous system. *J Comp Neurol* 248(4):475–517. <https://doi.org/10.1002/cne.902480404>
- Mena-Segovia J, Micklem BR, Ungless MA, Bolam JP (2009) GABAergic neuron distribution in the pedunculopontine nucleus defines functional subterritories. *J Comp Neurol* 515(4):397–408. <https://doi.org/10.1002/cne.22065>
- Mesulam MM, Mufson EJ, Wainer BH, Levey AI (1983) Central cholinergic pathways in the rat: an overview based on an alternative nomenclature Ch1-Ch6. *Neuroscience* 10(4):1185–1201. [https://doi.org/10.1016/0306-4522\(83\)90108-2](https://doi.org/10.1016/0306-4522(83)90108-2)
- Mesulam MM, Geula C, Bothwell MA, Hersh LB (1989) Human reticular formation: cholinergic neurons of the pedunculopontine and laterodorsal tegmental nuclei and some cytochemical comparisons to forebrain cholinergic neurons. *J Comp Neurol* 283(4):611–633. <https://doi.org/10.1002/cne.902830414>
- Mineff EM, Popratiloff A, Romansky R, Kazakos V, Kaimaktschieff V, Usunoff KG, Ovtsharoff W, Marani E (1998) Evidence for a possible glycinergic inhibitory neurotransmission in the midbrain and rostral pons of the rat studied by gephyrin. *Arch Physiol Biochem* 106(3):210–220. <https://doi.org/10.1076/apab.106.3.210.4377>
- Moro E, Hamani C, Poon Y-Y, Al-Khairyallah T, Dostrovsky JO, Hutchison WD, Lozano AM (2010) Unilateral pedunculopontine stimulation improves falls in Parkinson's disease. *Brain* 133(1):215–224. <https://doi.org/10.1093/brain/awp261>
- Mrak RE, Griffin WST (2007) Dementia with Lewy bodies: definition, diagnosis, and pathogenic relationship to Alzheimer's disease. *Neuropsychiatr Dis Treat* 3(5):619–625
- Müller ML, Bohnen NI (2013) Cholinergic dysfunction in Parkinson's disease. *Curr Neurol Neurosci Rep* 13(9):377. <https://doi.org/10.1007/s11910-013-0377-9>
- Nair-Roberts RG, Chatelain-Badie SD, Benson E, White-Cooper H, Bolam JP, Ungless MA (2008) Stereological estimates of dopaminergic, GABAergic and glutamatergic neurons in the ventral tegmental area, substantia nigra and retrorubral field in the rat. *Neuroscience* 152(4):1024–1031. <https://doi.org/10.1016/j.neuroscience.2008.01.046>

- Ogren SO, Kuteeva E, Elvander-Tottie E, Hökfelt T (2010) Neuropeptides in learning and memory processes with focus on galanin. *Eur J Pharmacol* 626(1):9–17. <https://doi.org/10.1016/j.ejphar.2009.09.070>
- Okada K, Nishizawa K, Kobayashi T, Sakata S, Kobayashi K (2015) Distinct roles of basal forebrain cholinergic neurons in spatial and object recognition memory. *Sci Rep* 5(1):13158. <https://doi.org/10.1038/srep13158>
- Oliveira VC, Carrara RC, Simoes DL, Saggiore FP, Carlotti CG Jr, Covas DT, Neder L (2010) Sudan black B treatment reduces autofluorescence and improves resolution of in situ hybridization specific fluorescent signals of brain sections. *Histol Histopathol* 25(8):1017–1024. [10.14670/HH-25.1017](https://doi.org/10.14670/HH-25.1017)
- Oorschot DE (1998) Total number of neurons in the neostriatal, pallidal, subthalamic, and substantia nigral nuclei of the rat basal ganglia: a stereological study using the cavalieri and optical disector methods. *J Comp Neurol* 366:580–599
- Orlowski RZ (1999) The role of the ubiquitin-proteasome pathway in apoptosis. *Cell Death Differ* 6(4):303–313. <https://doi.org/10.1038/sj.cdd.4400505>
- Paxinos G, Watson C (2009) *The rat brain in stereotaxic coordinates*. Elsevier Academic Press, San Diego
- Pienaar IS, Van de Berg W (2013) A non-cholinergic neuronal loss in the pedunculopontine nucleus of toxin-evoked parkinsonian rats. *Exp Neurol* 248:213–223. <https://doi.org/10.1016/j.expneurol.2013.06.008>
- Pienaar IS, Elson JL, Racca C, Nelson G, Turnbull DM, Morris CM (2013) Mitochondrial abnormality associates with type-specific neuronal loss and cell morphology changes in the pedunculopontine nucleus in Parkinson disease. *Am J Pathol* 183(6):1826–1840. <https://doi.org/10.1016/j.ajpath.2013.09.002>
- Pienaar IS, Harrison IF, Elson JL, Bury A, Woll P, Simon AK, Dexter DT (2015a) An animal model mimicking pedunculopontine nucleus cholinergic degeneration in Parkinson's disease. *Brain Struct Funct* 220(1):479–500. <https://doi.org/10.1007/s00429-013-0669-5>
- Pienaar IS, Gartside SE, Sharma P, De Paola V, Gretenkord S, Withers D, Elson JL, Dexter DT (2015b) Pharmacogenetic stimulation of cholinergic pedunculopontine neurons reverses motor deficits in a rat model of Parkinson's disease. *Mol Neurodegener* 10(1):47. <https://doi.org/10.1186/s13024-015-0044-5>
- Pienaar IS, Lee CH, Elson JL, McGuinness L, Gentleman SM, Kalaria EN, Dexter DT (2015c) Deep-brain stimulation associates with improved microvascular integrity in the subthalamic nucleus in Parkinson's disease. *Neurobiol Dis* 74:392–405. <https://doi.org/10.1016/j.nbd.2014.12.006>
- Pienaar IS, Vernon A, Winn P (2016) The cellular diversity of the pedunculopontine nucleus: relevance to behavior in health and aspects of Parkinson's disease. *Neuroscientist* 23(4):415–431. <https://doi.org/10.1177/1073858416682471>
- Pirondi S, Giuliani A, Del VG, Giardino L, Hökfelt T, Calza L (2010) The galanin receptor 2/3 agonist Gal2-11 protects the SN56 cells against beta-amyloid 25–35 toxicity. *J Neurosci Res* 88(5):1064–1073. <https://doi.org/10.1002/jnr.22278>
- Plaha P, Gill SS (2005) Bilateral deep brain stimulation of the pedunculopontine nucleus for Parkinson's disease. *Neuroreport* 16(17):1883–1887. <https://doi.org/10.1097/01.wnr.0000187637.20771.a0>
- Pope RJP, Holmes FE, Kerr NC, Wynick D (2010) Characterisation of the nociceptive phenotype of suppressible galanin overexpressing transgenic mice. *Mol Pain* 6:67. <https://doi.org/10.1186/1744-8069-6-67>
- Rinne JO, Ma SY, Lee MS, Collan Y, Røyttä M (2008) Loss of cholinergic neurons in the pedunculopontine nucleus in Parkinson's disease is related to the disability of the patients. *Parkinsonism Relat Disord* 14(7):553–557. <https://doi.org/10.1016/j.parkreldis.2008.01.006>
- Robinson TE, Becker JB (1982) Behavioral sensitization is accompanied by an enhancement in amphetamine-stimulated dopamine release from striatal tissue in vitro. *Eur J Pharmacol* 85(2):253–254. [https://doi.org/10.1016/0014-2999\(82\)90478-2](https://doi.org/10.1016/0014-2999(82)90478-2)
- Salio C, Lossi L, Ferrini F, Merighi A (2006) Neuropeptides as synaptic transmitters. *Cell Tissue Res* 326(2):583–598. <https://doi.org/10.1007/s00441-006-0268-3>
- Skofitsch G, Jacobowitz DM (1985) Immunohistochemical mapping of galanin-like neurons in the rat central nervous system. *Peptides* 6(3):509–546. [https://doi.org/10.1016/0196-9781\(85\)90118-4](https://doi.org/10.1016/0196-9781(85)90118-4)
- Steiner RA, Hohmann JG, Holmes A, Wrenn CC, Cadd G, Jureus A, Clifton DK, Luo M, Gutshall M, Ma SY, Mufson EJ, Crawley JN (2001) Galanin transgenic mice display cognitive and neurochemical deficits characteristic of Alzheimer's disease. *Proc Natl Acad Sci U S A* 98:4194–4189
- Tatemoto K, Rökaeus Å, Jörnvall H, McDonald TJ, Mutt V (1983) Galanin: a novel biologically active peptide from porcine intestine. *FEBS Lett* 164(1):124–128. [https://doi.org/10.1016/0014-5793\(83\)80033-7](https://doi.org/10.1016/0014-5793(83)80033-7)
- Taylor CL, Kozak R, Latimer MP, Winn P (2004) Effects of changing reward on performance of the delayed spatial win-shift radial maze task in pedunculopontine tegmental nucleus lesioned rats. *Behav Brain Res* 153(2):431–438. <https://doi.org/10.1016/j.bbr.2003.12.019>
- Vernon A, Johansson S, Modo M (2010) Non-invasive evaluation of nigrostriatal neuropathology in a proteasome inhibitor rodent model of Parkinson's disease. *BMC Neurosci* 11(1):1. <https://doi.org/10.1186/1471-2202-11-1>
- Vrontakis ME (2002) Galanin: a biologically active peptide. *Curr Drug Targets CNS Neurol Disord* 1(6):531–541. <https://doi.org/10.2174/1568007023338914>
- West MJ, Slomianka L, Gundersen HJ (1991) Unbiased stereological estimation of the total number of neurons in the subdivisions of the rat hippocampus using the optical fractionator. *Anat Rec* 231(4):482–497. <https://doi.org/10.1002/ar.1092310411>
- Wraith DC, Pope R, Blutzkueven H, Holder H, Vanderplank P, Lowrey P, Day MJ, Gundlach AL (2009) A role for galanin in human and experimental inflammatory demyelination. *Proc Natl Acad Sci U S A* 106(36):15466–15471. <https://doi.org/10.1073/pnas.0903360106>
- Zhang L, Yu W, Schroedter I, Kong J, Vrontakis M (2012) Galanin transgenic mice with elevated circulating galanin levels alleviate demyelination in a cuprizone-induced MS mouse model. *PLoS One* 7(3):e33901. <https://doi.org/10.1371/journal.pone.0033901>
- Zhou HY, Tan YY, Wang ZQ, Wang G, Lu GQ, Chen SD (2010) Proteasome inhibitor lactacystin induces cholinergic degeneration. *Can J Neurol Sci* 37(02):229–234. <https://doi.org/10.1017/S0317167100009975>